



$Z \rightarrow \mu\mu$ performance with the Upgraded ATLAS Tracker for HL-LHC

Khrystyna Gnatenko
Lviv Franko National University, Ukraine

DESY ATLAS Group
Supervisors: Peter Vankov, Tiago Perez

6th September 2012, Hamburg

Abstract

In order to fully profit from the LHC potential, the luminosity of the machine will be increased. This upgrade project is called High-Luminosity LHC and is expected to take place in ~ 2022 .

In this document, the results of a study $Z \rightarrow \mu\mu$ performance with the Upgraded ATLAS Tracker (ITk) for High-Luminosity LHC are presented. The possibility to reconstruct invariant mass is considered with no pileup conditions and also with some complications: high-pileup conditions, large track multiplicity.

Contents

1	Introduction	3
2	Physics Motivations for the HL-LHC Upgrade	3
3	Current ATLAS Inner Detector	4
4	Motivation for ATLAS ID upgrade for HL-LHC	5
5	ITk-LoI (Letter of Intent) layout	6
6	Simulation description and Analysis	7
6.1	Athena framework	7
6.2	Pileup events simulation	8
7	Results	8
7.1	Event displays (ITk-LoI)	8
7.2	Analysis developed for $Z \rightarrow \mu\mu$ reconstruction using truth information . .	10
8	Summary	23

1 Introduction

ATLAS [1] is a high-energy physics experiment at the Large Hadron Collider (LHC) at CERN [2].

The ATLAS detector is shaped of four major components: inner detector, calorimeter, muon spectrometer, magnet system. It is designed to explore the proton-proton collisions with a center of mass energy of $\sqrt{s} = 14\text{TeV}$ at a maximum luminosity of $L_{peak} = 10^{34}\text{cm}^{-2}\text{s}^{-1}$.

It has been decided that LHC will be upgraded to High-Luminosity LHC (denoted HL-LHC) in ~ 2022 .

The luminosity of the HL-LHC is expected to reach $L_{peak} \geq 5 \cdot 10^{34}\text{cm}^{-2}\text{s}^{-1}$. HL-LHC will accumulate an integrated luminosity of $L_{int} \sim 3000\text{fb}^{-1}$. It is predicted that the mean number of interactions per bunch crossing will be $\langle N_{int} \rangle \sim 140$ [3]. Currently LHC works at $\langle N_{int} \rangle \sim 25$. The centre of mass energy will be kept at the nominal $\sqrt{s} = 14\text{TeV}$. New technologies will be developed for HL-LHC: high field magnets, electrical transfer lines, e.t.

High-luminosity conditions give a lot of new possibilities for physics studies but they are also very challenging experimentally due to high track multiplicity and the level of radiation damage. So, to make the ATLAS detector suitable for operation in that environment, an upgrade is required.

2 Physics Motivations for the HL-LHC Upgrade

The main physics motivations for the HL-LHC are to make precision measurements of the Standard Model and to explore the physics beyond it. It is expected that HL-LHC will perform [4]:

- More accurate measurements on the new particles discovered at the LHC;
- Detailed studies of:
 - Higgs properties;
 - SUSY (if discovered) parameters, properties of SUSY particles (mass, decay, etc.) channels;
- Explore the gauge structure of the SM;
- Extending the exploration of the energy frontier;
- Studies rare processes with rates below the sensitivity of current phase;
- Extending the exploration of the energy frontier;
- Studies rare processes with rates below the sensitivity of current phase;
- Strong electroweak symmetry breaking;

- Extra dimensions;
- Other phenomena (if any exist).

3 Current ATLAS Inner Detector

The basic task of the Atlas Inner Detector (denoted throughout this report by ID) is to track charged particles from the beam-pipe to the calorimeter system. That is possible due to detecting particular interaction with material at discrete points. Also, the information of the ID is used to determine particle momentum and the types of certain particles.

The Atlas Inner Detector is composed of pixel detector (PD), semiconductor tracker (SCT, silicon microstrips) and transition radiation tracker (TRT, gaseous straw tubes), Fig. 1. All of them are contained in the Central Solenoid, which provides a nominal magnetic field of 2 T [5].

Charged particles are caused by magnetic field to curve in a direction that reveals their charge. The momentum of particles is revealed by the curvatures degree. Vertex reconstruction and electron identification are also possible.

The innermost part of the ID is the Pixel Detector (PD). It has three discs, which are located on each end-cap and three concentric layers. The challenge is the radiation to which the PD is exposed because of its proximity to the interaction point. So, in order to provide a long period running all components have to be radiation hardened.

Mane PD function is to provide engineering challenge high-precision set of measurements in very close to the interaction point region. The Pixel Detector has over 80 million read-out channels.

Semi-Conductor Tracker (SCT) is the middle component of the ID and the most critical ID's part for basic tracking in the plane perpendicular to the beam. It is designed to provide measurements of impact parameter, momentum and vertex position. SCT cover larger area than PD but in its functions and concepts it is similar to PD. [6].

The outermost component of the inner detector is the Transition Radiation Tracker (TRT). Drift tubes (straws) are the detecting elements. They are 4 mm in diameter and up to 144 cm long.

The barrel contains about 50000 straws, 320000 radial straws are contained in the end-caps [7]. When a charged particle passes through the straw the gas in it becomes ionized. The path of the particle can be determined due to pattern of hit straws created by the wires with signals.

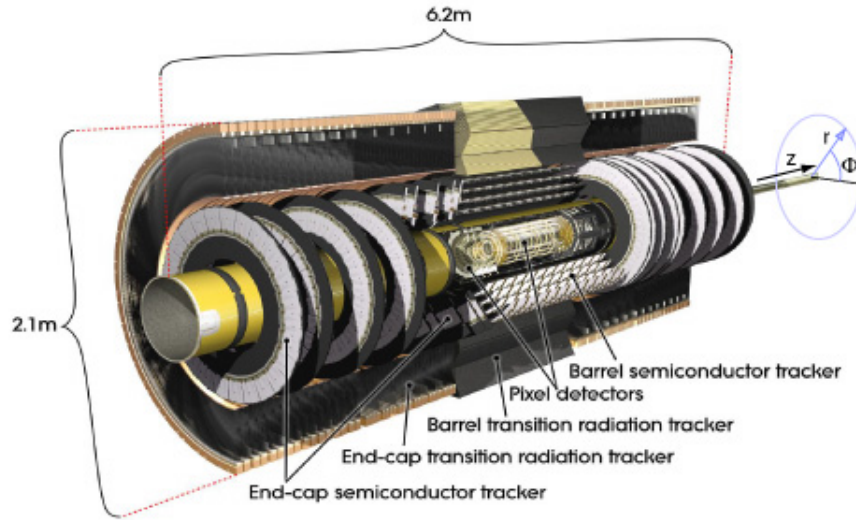


Figure 1: current ATLAS Inner Detector.

4 Motivation for ATLAS ID upgrade for HL-LHC

There are a lot of factors that make the upgrade of the ATLAS Inner Detector required. The most important are:

- detector elements and electronics has to be sufficiently radiation hard.
- necessity of running for a long periods at the increased luminosity, without replacement of components every few years.
- increase of pile-up events, resulting in higher detector occupancies, which are beyond the TRT design parameters.

Therefore, for the ATLAS Inner Detector to still be effective, it has to be completely replaced by a new system fully built of silicon detectors, without TRT [8]. The upgrade of the LHC and respectively of the ATLAS experiment is expected to develop (emanate) in three phases.

Phase 0 is predicted to take place in 2013-2014. During this two years the ATLAS Collaboration has decided to:

- add new, 4th pixel layer (IBL) which will be located between the innermost pixel layer and the beam pipe in the Pixel detector. This additional layer will boost the tracking performance, extending the reach of the physics analysis.
- put new beam pipe made of aluminum to reduce the backgrounds by a factor of 10-20. Such background decrease could not be achieved without upgrade of the new beam pipe.
- replace the ID cooling system;

- complete the muon system;
- put new neutron shielding.

The time range of the Phase 1 is 2017-2018. In this phase the peak luminosity is expected to increase to $2 \cdot 10^{34} \text{cm}^{-2} \text{s}^{-1}$. Also, it is foreseen:

- to install New Muon small wheels;
- to improve level-2 triggers (Fast TracKer project (FTK) topological triggers) That gives major improvement for b-tagging and lepton isolation.

The last step is Phase 2 (2022-). Upgrade to enable HL-LHC. $L_{peak} \geq 5 \cdot 10^{34} \text{cm}^{-2} \text{s}^{-1}$. To make the ATLAS detector suitable to this conditions it is necessary to install:

- new Inner detector (ITk) completely made of silicon;
- upgrade of the Forward Calorimeter;
- new electronics for the Liquid Argon calorimeter;
- changes to the Muon system.

5 ITk-LoI (Letter of Intent) layout

The "Letter of Intent" ITk layout (ITk-LoI), was developed in order to create a baseline design for a tracker for Phase-2. The ITk-LOI-layout is based on the previous layout so-called UTOPIA and was designed to address its disadvantages.

The ITk-LOI-layout is implemented into Geant4 for detailed performance studies and also studies of physics processes relevant to HL-LHC operation. At the same time, it is used as a basis for detailed engineering studies, service optimizations, etc.

The LoI-layout is composed of two subsystems, using:

1. silicon pixel sensor technology
2. silicon microstrips.

The structure of ITk-LoI is shown in Fig. 2. The pixel and silicon micro-strip sub-detectors are independent. The pixel sub-detector has 4 barrel layers with 6 endcap disks. The range of barrel layers radii is from 39 mm (inner barrel layer) to 250 mm (outer layer). Endcap discs are located at z-positions from 877 mm to 1675 mm.

The strip sub-detector surround the pixel system and has 5 barrel layers and a barrel "stub cylinders", intended to fill a coverage gap between the barrels and endcaps. The radii of full length barrel layers is from 405 mm to 1000 mm. Barrel "stub cylinders" are placed at either end of the barrel between the fourth and fifth full layers. They are similar to the long strip barrel but only 2 modules long rather than 13. The length of strips used in barrel layers is different: the three inner layers has strips of 23.82 mm; the length of strips in the outer two layers and stub cylinders is 47.64 mm. A strip pitch of

$75\mu\text{m}$ is used throughout the barrel. Every layer provides two "hits" because strip sensors are double sided (with a 40 mrad stereo angle rotation). In the track reconstruction this two hits are combined into a single "space point".

The strip sub-detector is also complemented by 7 disks in each end-cap at z-positions between 1415 mm and 3000 mm.

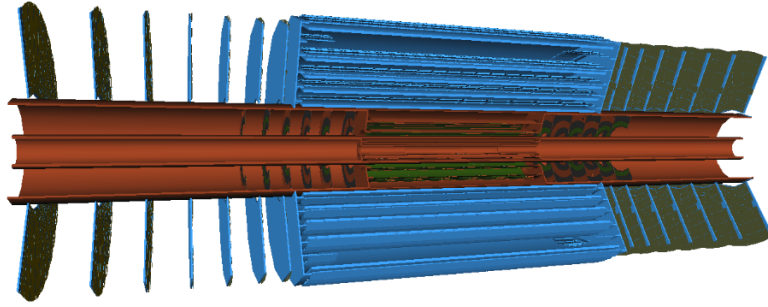


Figure 2: LoI layout.

6 Simulation description and Analysis

6.1 Athena framework

The simulation, reconstruction and analysis are performed within Athena, common framework used by the ATLAS experiment [9]. It is designed to model the interaction of particles, to simulate and digitize the data that is fully compatible with ATLAS offline reconstruction. For the most part of these studies the Monte-Carlo production chain is used. [10].

The simulation and reconstruction implemented in the Athena framework follow four stages:

1. Event generation(Pythia event generator is used);
2. Simulation;
3. Digitization (detector response);
4. Reconstruction of the particle track.

Geant4 is used to simulate energy losses of the particle passing through the detector volume and the secondary particle creation, its propagation [11]. In order to define the design of detector and detector elements GeoModel package is used, which interface with the GeoModel package. The next step is digitization. It provides conversion of the energy losses to the detector electronic response. It is possible due to assigning of every readout channel with unique address. To store this address 32-bit identifiers are used. But it is

not enough for ATLAS Inner Tracker following upgrade because of extending the number of channels desired in the new Inner Tracker. So it is necessary to exploit the 64-bit word. Reconstruction include creation of the particular tracks from the space point information and restoration of the simulated data.

6.2 Pileup events simulation

Following LHC upgrade a new beam conditions will be provided. The HL-LHC beams are expected to produce an average of 140 interactions each time they cross because of linear scaling of the average number of interactions created in a bunch crossing with luminosity [12]. That's why the simulation of a large number of additional pile-up events is required.

Pile-up interactions are randomly picked from sets of minimum bias events. This events are simulated in the same way to the signal and generated with the help of Pythia 8 - computer simulation program for particle collisions at very high energies.

The pile-up collisions will overlay the simulation of the signal process.

7 Results

In this project we concentrated on one of the easiest detectable Z-boson decay-mode – the decay into muon-antimuon.

Z boson is neutral particle with $Mass = 91.1876 \pm 0.0021 GeV$. It is an momentous ingredient in many SM ($H \rightarrow ZZ$) and new physics processes. Precise Z boson reconstruction is vital.

Z boson is a short-lived particle with the half-life of about $3 \cdot 10^{-25} s$. In 10% of the Z-decays, charged lepton-antilepton pairs are produced; in 20% of the cases the Z boson decays into a neutrino-antineutrino pair; a quark-antiquark pair is produced in 70% of Z decays. Also Z-boson can decay into a fermion and its antiparticle the example of which mode we considered.

We have studied $Z \rightarrow \mu\mu$ performance with the LoI-ITk and examined possibility to reconstruct invariant mass under different conditions (with and without high-pileup).

7.1 Event displays (ITk-LoI)

With the help of Athena Software framework we have done all steps of the Monte-Carlo production chain: event generation (using job option MC11.106047.PythiaZmumu_no_filter.py), simulation, digitization, reconstruction of the particle track for high-pileup of 140 and without pileup.

In Fig. 3 and Fig. 4 the event displays without pileup and with pileup of 140 are presented. This displays reflect the ITk-LoI layout. They are made with VP1 after the full simulation cycle.

It can be seen that there is a significant difference in the number of tracks between the event displays with pileup 140 and without pileup. In Fig. 3 it is easy to see two muon candidates, represented in green color. But it is not an easy task to find two muon candidates because of significantly large number of tracks.

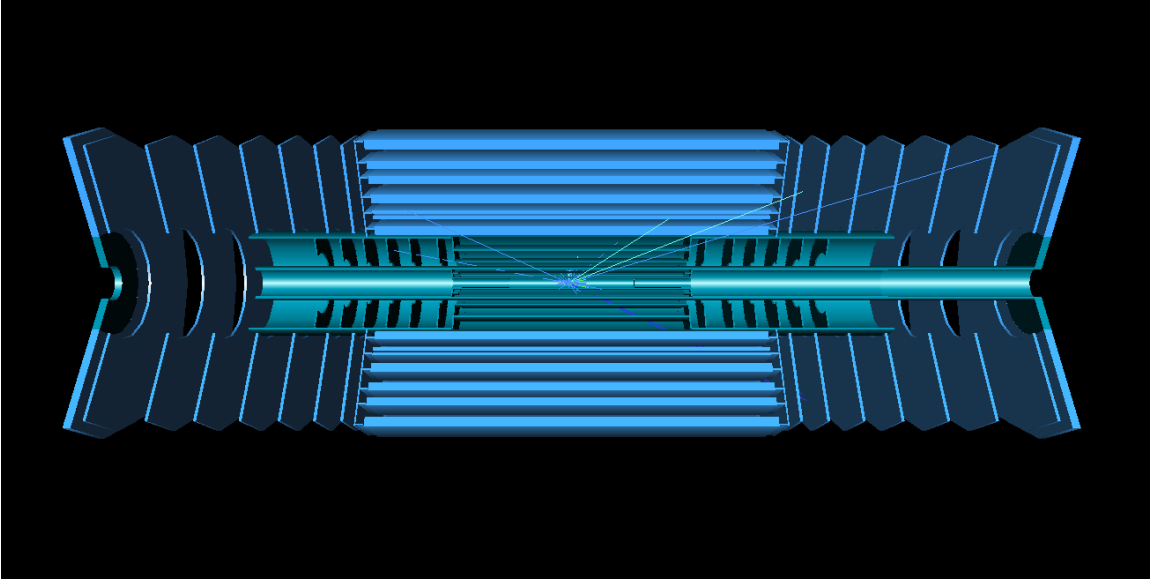


Figure 3: Event display without pileup.

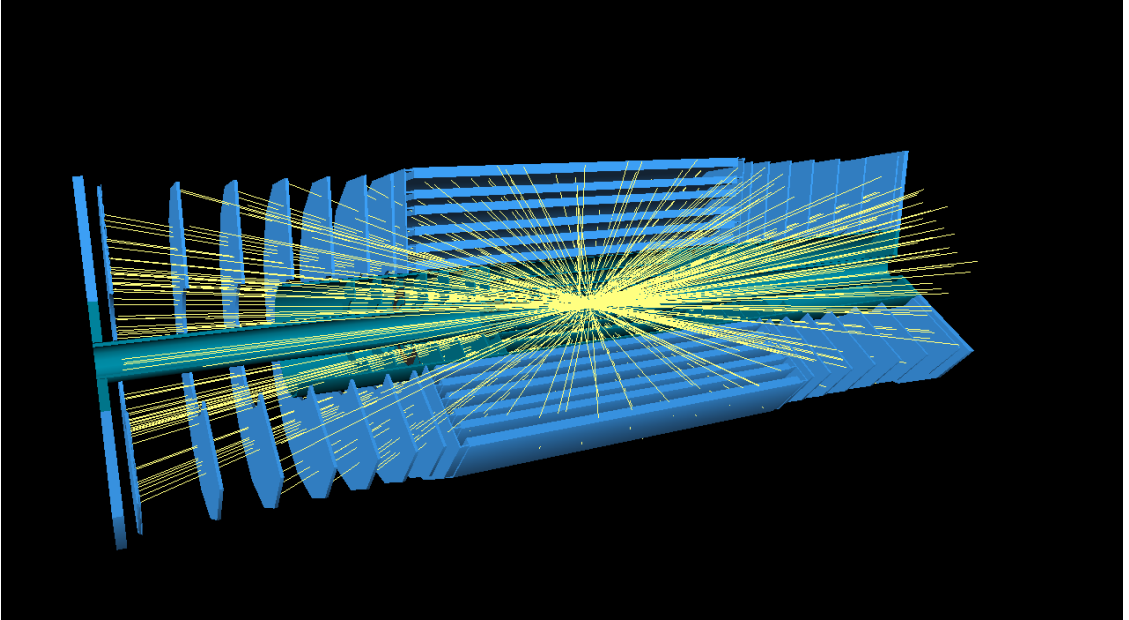


Figure 4: Event display with pileup 140.

7.2 Analysis developed for $Z \rightarrow \mu\mu$ reconstruction using truth information

In this project analysis developed for $Z \rightarrow \mu\mu$ reconstruction was developed. ITk standalone is used.

There is no way to distinguish our muon candidates by using only reco NTUP, since we don't have information from Muon Spectrometer. So, the reconstruction of the invariant mass requires linking reco to truth data sets. Therefore, to find invariant mass estimate we have to do the following steps:

1. Apply the cuts for truth candidates:
 - We require that longitudinal impact parameter to be less than 150 mm and transverse impact parameter to be less than 1 mm.
 - The pseudorapidity $\eta = -\ln(\tan \frac{\theta}{2})$ has to be less than 2.5.
 - We also apply cut on particle barcode – a number that identifies a particle within an event. Requiring barcode of the truth candidate to be different from 0 and less than 100000, we exclude particles generated from Geant.
 - The cut on p_t is also used. We expected to have muon candidates with high p_t .
2. Find the reco track with the best matching associated to the truth track. We require that the reconstructed track matches a truth particle with a probability greater than 0.5.
3. Apply cuts to the reco candidates
 - We apply the cut of hits number – the total number of hits on track in all layers (pixel + Si-strip). The candidate track has to have at > 9 hits ($pixHits + sctHits \geq 9$).
 - Longitudinal and transverse impact parameters are also used as a cuts
4. Build muon pairs from reco muon candidates with opposite charge.
5. Find the invariant mass by using:

$$M^2 = 2p_t^1 \cdot p_t^2 (\cosh(\eta_1 - \eta_2) - \cos(\varphi_1 - \varphi_2))$$

6. Look in invariant mass window of $[70, 120]$ GeV. The position of resonance peak is expected to be close to the Z bosons mass.
7. The last step is to fit the plots with Breit-Wigner function:

$$BW(x) = \frac{1}{2\pi} \frac{I_0 \Gamma}{(x - M_0)^2 + 0.24 \Gamma_0^2}$$

To find the power of all cuts, we applied, a cutflow table was constructed. Large decrease of number of tracks after applying the p_t cut leads to a conclusion: the most powerful cut which helps to get clear Z peak is cut on p_t .

Cutflow was constructed for two cases: $p_t > 5$ and $p_t > 20$. For both cuts, as it is shown in the Tab. 1, a large decrease of tracks number even with pileup 140 takes place.

	no pileup	pileup of 140
total	383456	13999110
z0Cut = 150	382982	13907180
d0Cut=1	377511	13629410
η Cut=2.5	359441	12910230
matchCut=0.5	359393	12904470
hitsCut=9	359393	12904470
PtCut=20 GeV	29016	30349
PtCut=5 GeV	49009	157193

Table 1: Cutflow.

Therefore, we applied different p_t cuts: 5GeV, 15GeV, 20GeV, 25GeV and 30GeV. In the Fig. 5 and Fig. 6, the transverse momentum and pseudorapidity distributions of two muon candidates with p_t cut of 5GeV are shown. The red color responds to no pileup and the green colour – pileup-140.

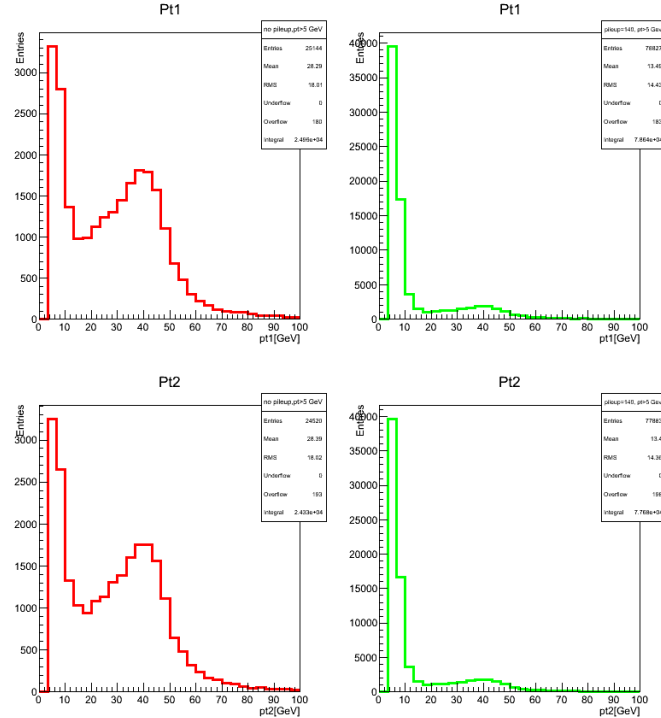


Figure 5: p_t distribution of two muon candidates, p_t cut 5GeV, no pileup (red), pileup 140 (green).

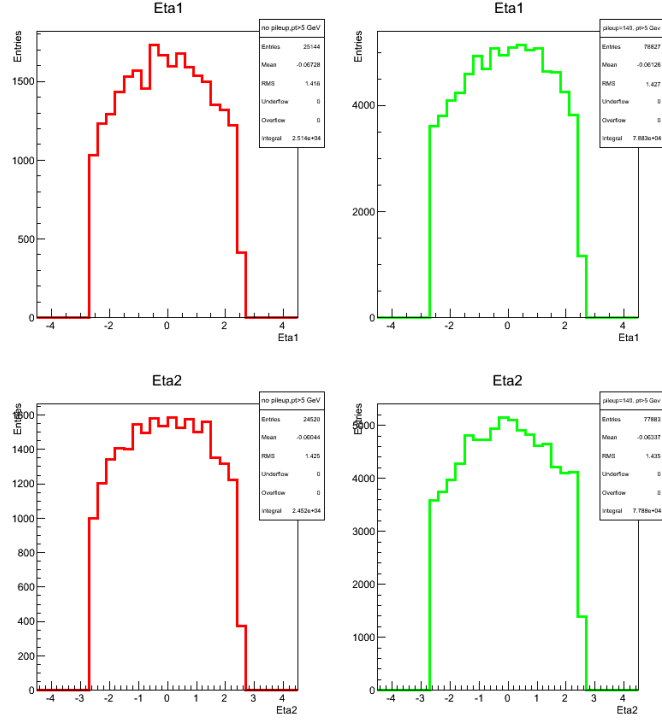


Figure 6: η distribution of two muon candidates, p_t cut 5 GeV, no pileup (red), pileup 140 (green).

Reconstruction of invariant Mass with $p_t > 5$ does not bring a clear resonans peak, especially in presence of pileup. This can be seen in Fig. 7. But the resonance peak exists. It is possible to fit close to the resonance range with Breit-Wigner function, as it is presented in Fig. 8.

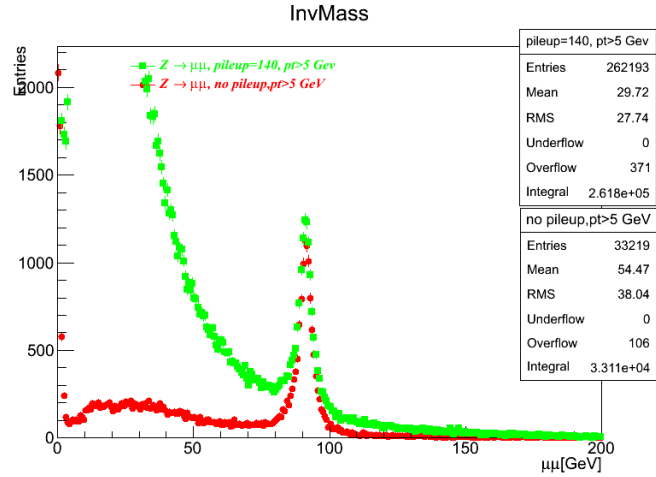


Figure 7: Invariant Mass of two muon candidates, p_t cut 5 GeV, no pileup (red), pileup 140 (green)

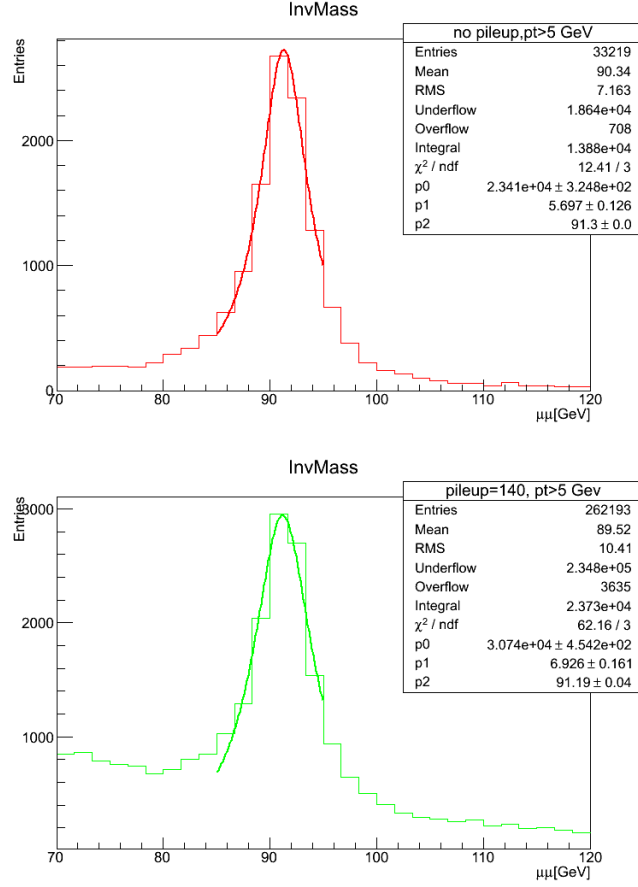


Figure 8: Fitting Invariant Mass with Breit-Wigner.

Next step was to apply stronger cuts on p_t . In Fig. 9 and Fig. 10 p_t and η distributions of two muon candidates with $p_t > 15\text{GeV}$ can be seen. The same distributions, but with another cut $p_t > 20\text{GeV}$ are shown in Fig. 13 and Fig. 14. Also we have plotted transverse momentum and pseudorapidity distribution for $p_t > 25\text{GeV}$ and $p_t > 30\text{GeV}$ in Fig 17, Fig 18 and Fig. 21, Fig. 22, respectively. In all these cases with different cuts we obtained a clear peak in very close position to the expected Z-boson mass. The significant difference between results is only in value of Z mass resolution (σ). Increasing the p_t cut provides decreasing in σ . The results of invariant mass reconstruction are shown in the Fig. 11, Fig 12 (15 GeV); Fig. 15 Fig. 16 (20 GeV); Fig. 19, Fig 20. (25 GeV); and Fig. 23, Fig 24 (30GeV).

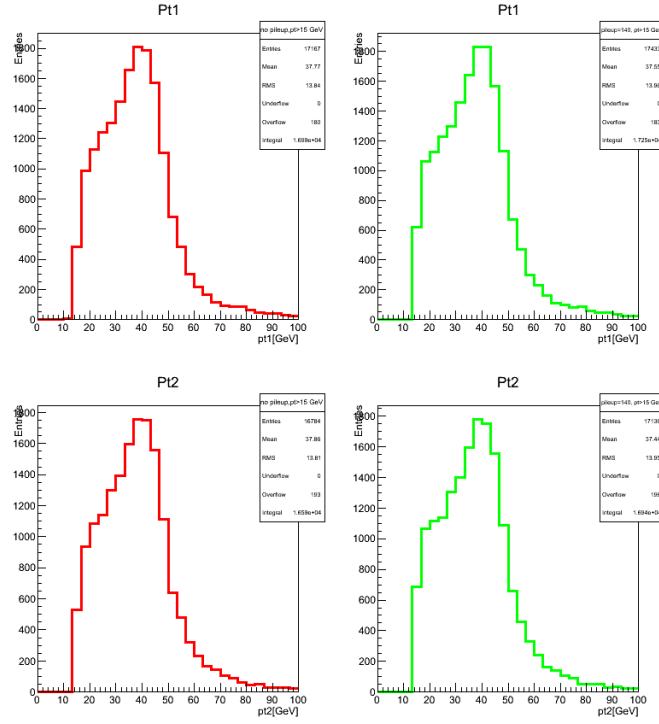


Figure 9: p_t distribution of two muon candidates, p_t cut 15GeV, no pileup (red), pileup 140 (green).

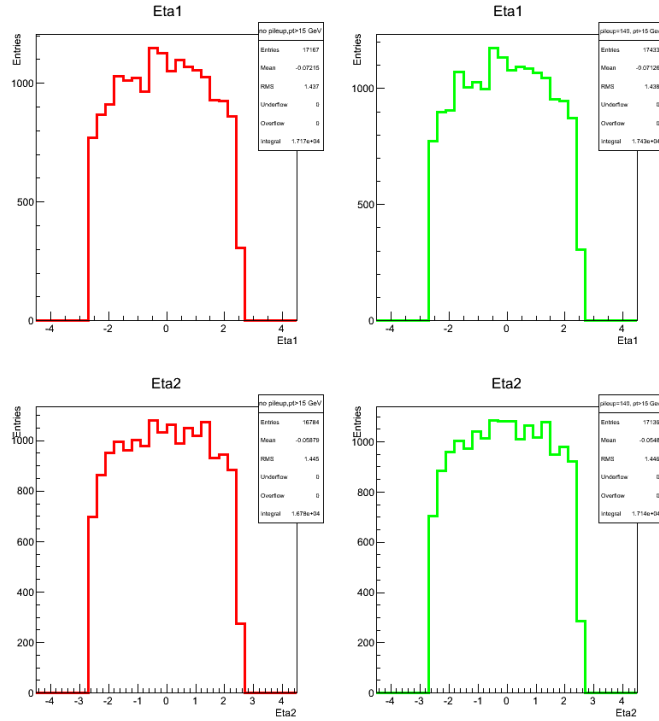


Figure 10: η distribution of two muon candidates, p_t cut 15GeV, no pileup (red), pileup 140 (green).

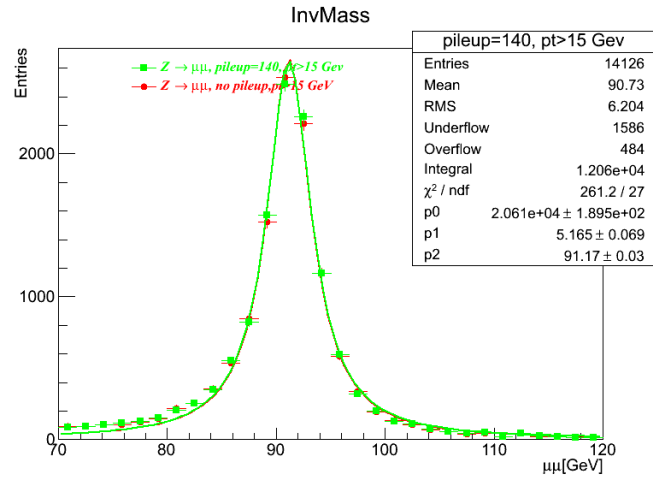


Figure 11: Invariant Mass of two muon candidates, p_t cut 15GeV, no pileup (red), pileup 140 (green)

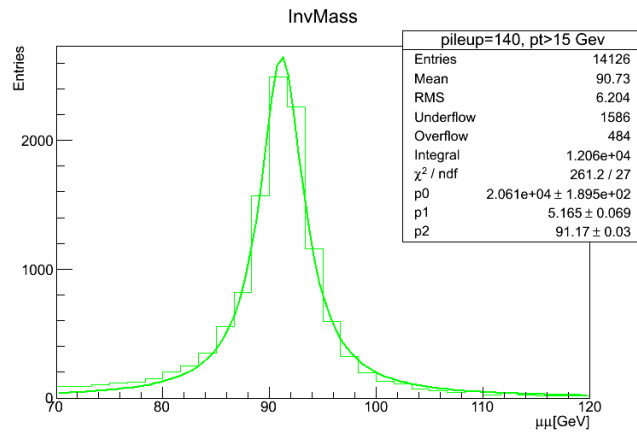
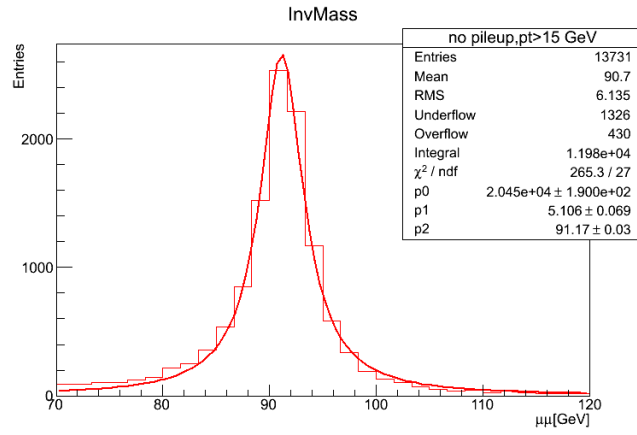


Figure 12: Fitting Invariant Mass with Breit-Wigner.

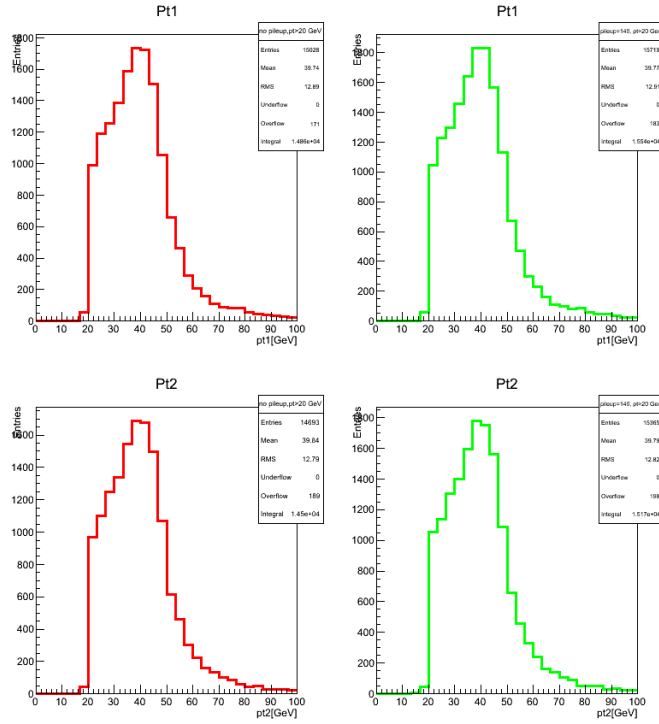


Figure 13: p_t distribution of two muon candidates, p_t cut 20GeV, no pileup (red), pileup 140 (green).

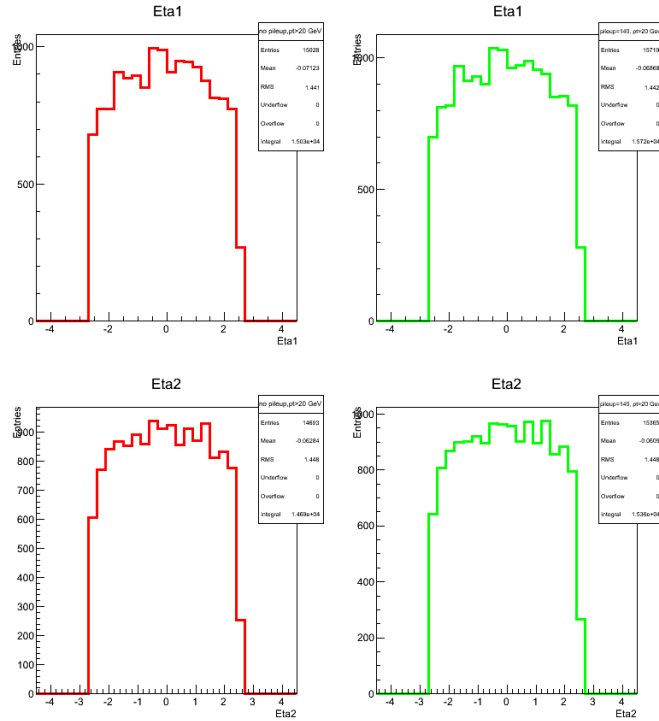


Figure 14: η distribution of two muon candidates, p_t cut 20GeV, no pileup (red), pileup 140 (green).

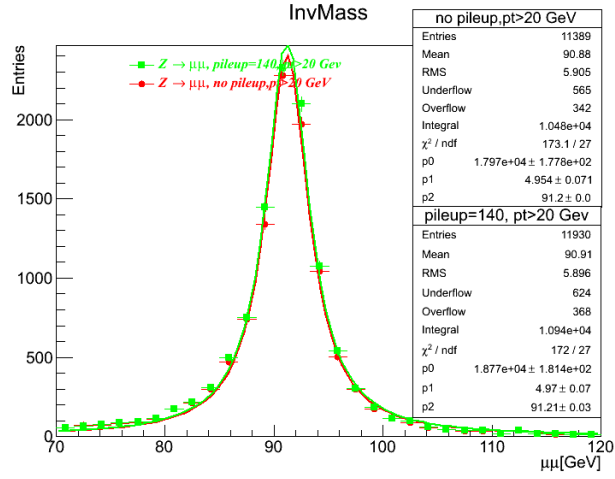


Figure 15: Invariant Mass of two muon candidates, p_t cut 20GeV, no pileup (red), pileup 140 (green)

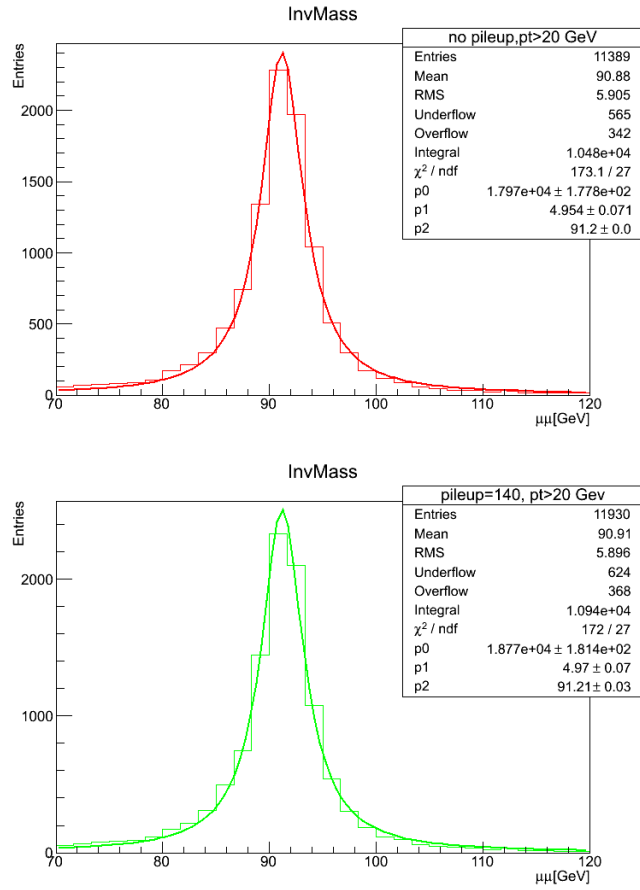


Figure 16: Fitting Invariant Mass with Breit-Wigner.

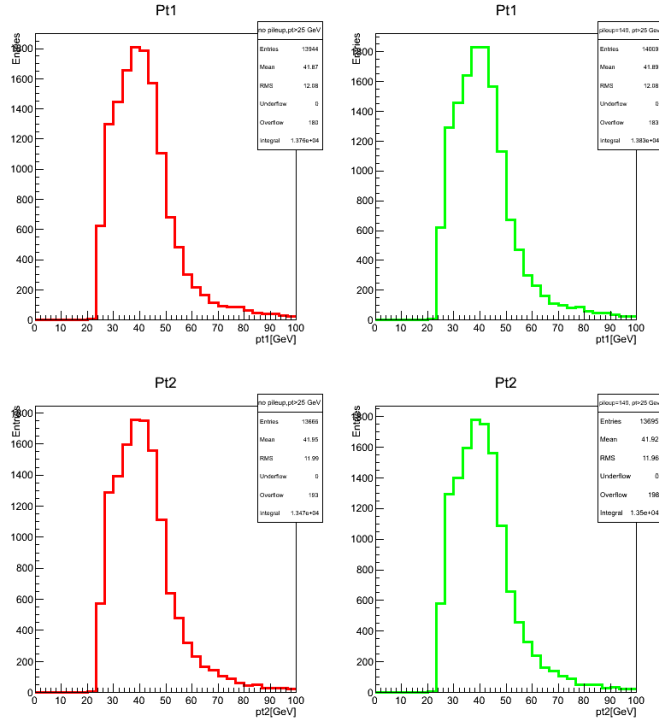


Figure 17: p_t distribution of two muon candidates, p_t cut 25GeV, no pileup (red), pileup 140 (green).

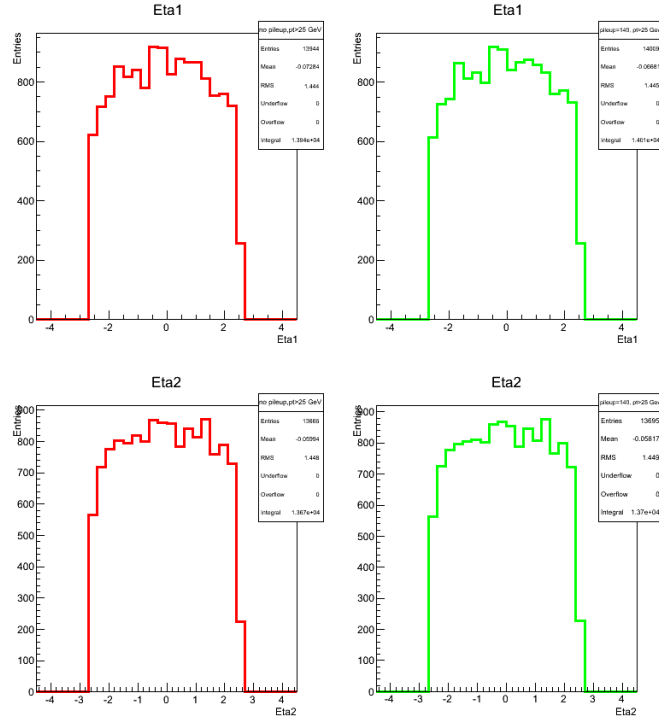


Figure 18: η distribution of two muon candidates, p_t cut 25GeV, no pileup (red), pileup 140 (green).

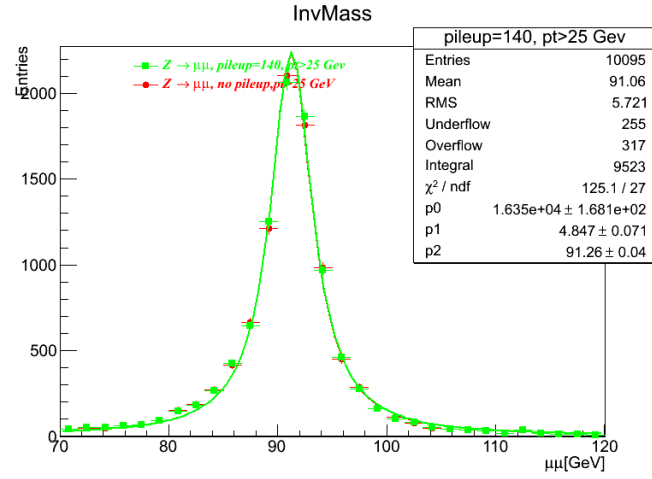


Figure 19: Invariant Mass of two muon candidates, p_t cut 25GeV, no pileup (red), pileup 140 (green)

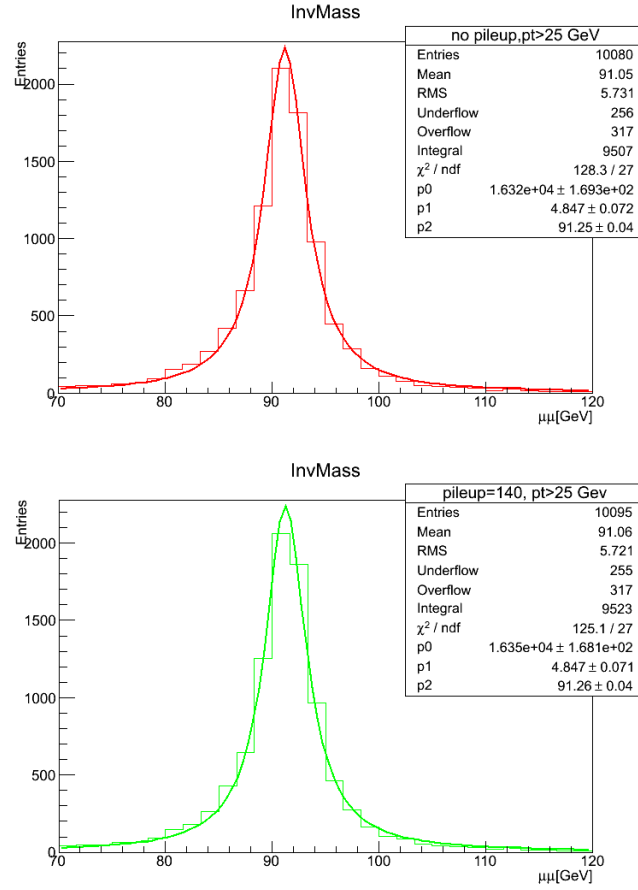


Figure 20: Fitting Invariant Mass with Breit-Wigner.

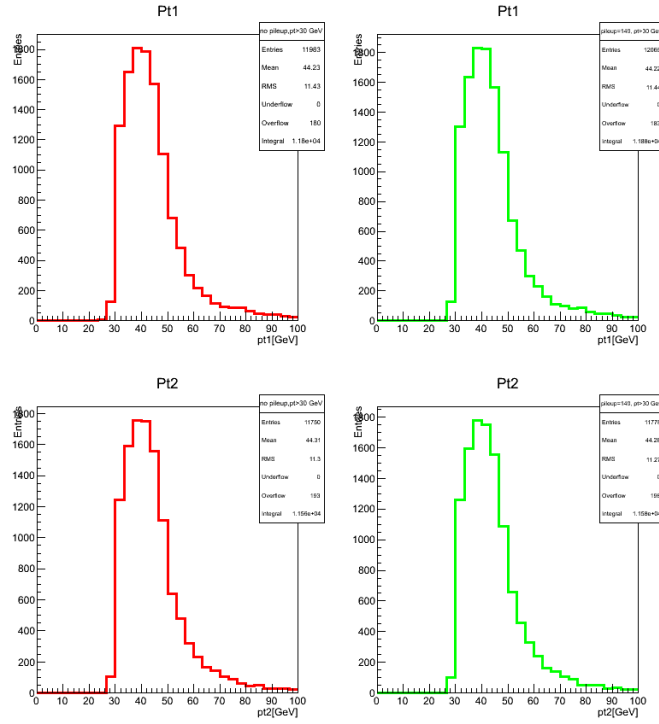


Figure 21: p_t distribution of two muon candidates, p_t cut 30GeV, no pileup (red), pileup 140 (green).

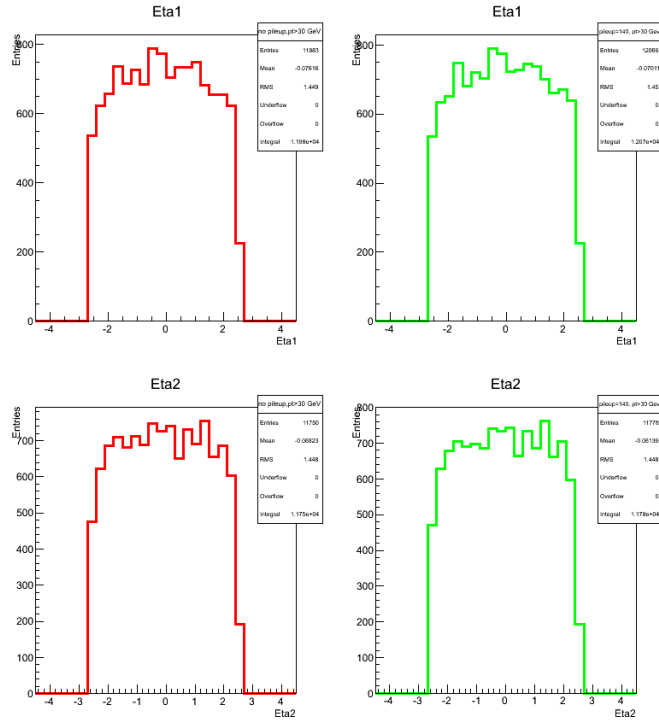


Figure 22: η distribution of two muon candidates, p_t cut 30GeV, no pileup (red), pileup 140 (green).

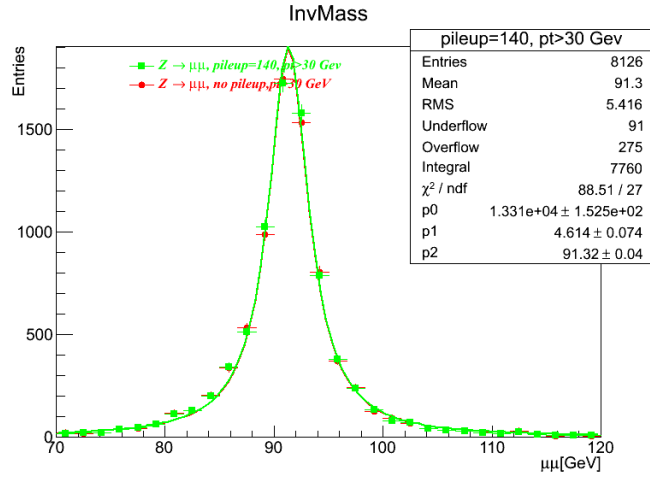


Figure 23: Invariant Mass of two muon candidates, p_t cut 30 GeV, no pileup (red), pileup 140 (green)

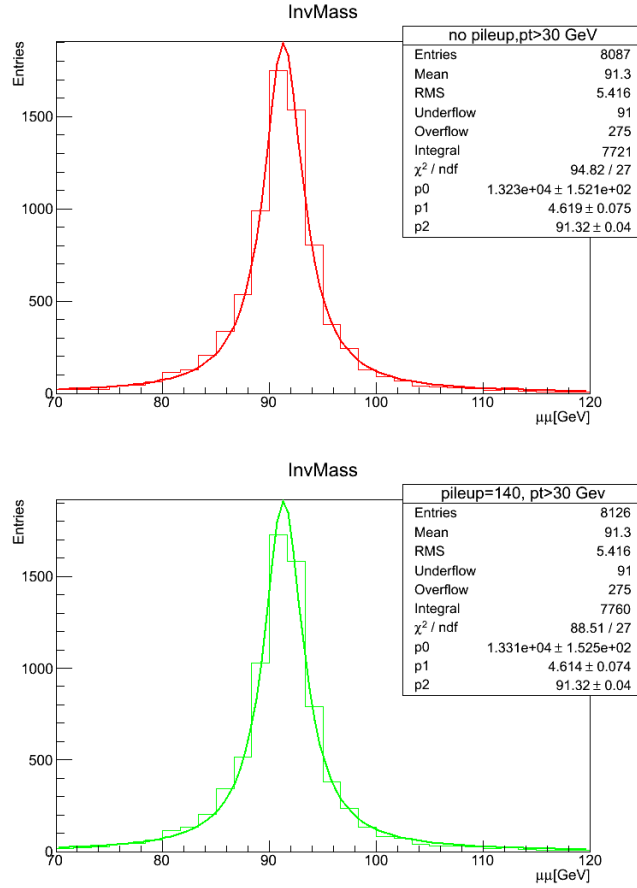
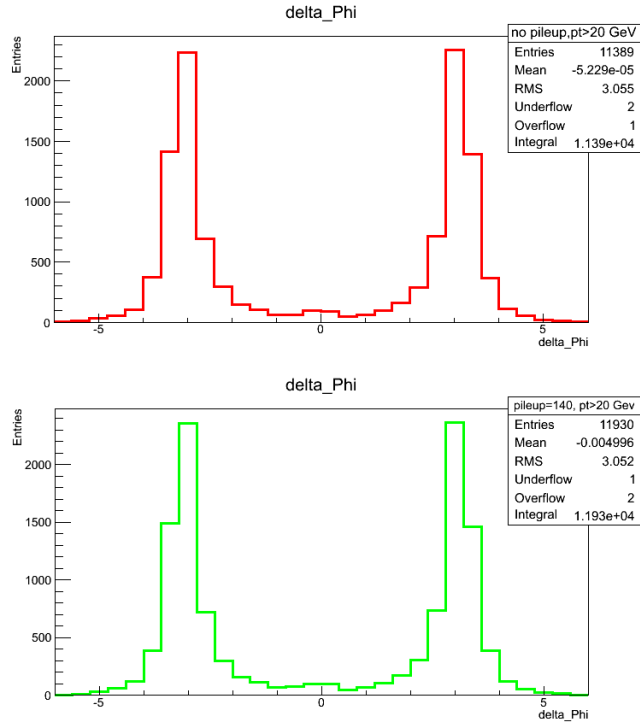
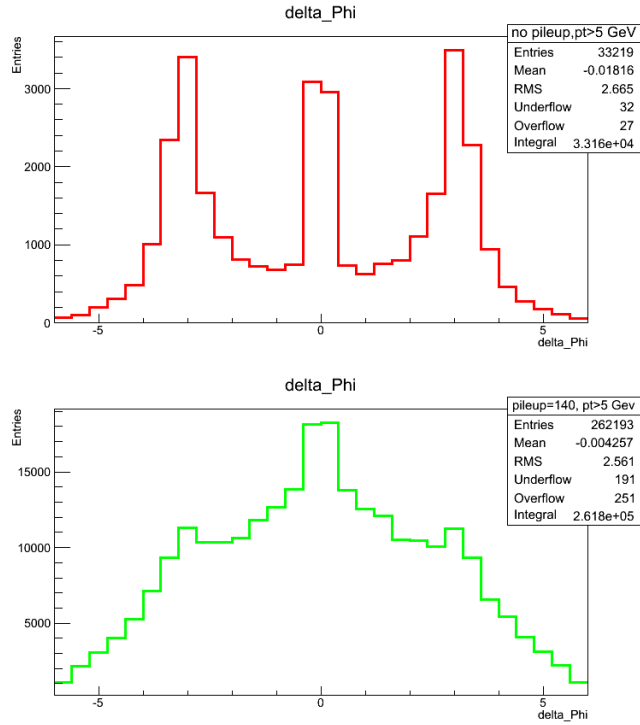


Figure 24: Fitting Invariant Mass with Breit-Wigner.

The distribution of $\varphi_1 - \varphi_2$ (φ_1 and φ_2 angles respective particle candidates with opposite charge) leads to a conclusion: with p_t cut 20 GeV angle between muon candidates is very close to π .



$\Delta\varphi$ distribution of two muon candidates, p_t cut 20 GeV, no pileup (red), pileup 140 (green)



$\Delta\varphi$ distribution of two muon candidates, p_t cut 5 GeV, no pileup (red), pileup 140 (green)

8 Summary

ATLAS ITk upgrade is an important and active area of research.

In this project, the $Z \rightarrow \mu\mu$ performance with the LoI-ITk under HL-LHC conditions has been studied.

In our analysis developed for $Z \rightarrow \mu\mu$ reconstruction we used MC-truth information. Z-boson invariant mass was constrained using of p_t cuts 5, 15, 20, 25, 30 GeV under the different conditions: pileup-140 and without pileup. The cutflow showed that p_t cut is the most powerful cut that helped to get a clear Z peak with no pileup and with pileup-140. The results we obtained leads to a conclusion that applying p_t , barcode, pseudorapidity and impact parameters cuts gives a clear pick without pileup and even with pileup 140. One of the further possible improvements is inclusion of SM backgrounds, which gives the possibility of comparison with current ATLAS, etc.

References

- [1] G. Aad, *et al.*, *The ATLAS Experiment at the CERN Large Hadron Collider*, J. Instr. 3 (2008) S08003.
- [2] L. Evans and P. Bryant, *LHC Machine*, J. Instr. 3 (2008) S08001.
- [3] P. Allport, *ATLAS tracking at the super-LHC*, Nucl. Instrum. Meth. A579 (2007) 592-594.
- [4] G.Azuelos et al., *Physics in ATLAS at a Possible Upgraded LHC*, ATL-COM-PHYS-2000-030, March 2001.
- [5] ATLAS Collaboration, *Inner Detector Technical Design Report vol. I & II*, CERN/LHCC/97-16 & CERN/LHCC/97-17 (1997).
- [6] A. Abdesselam, *et al.*, *The Barrel Modules of the ATLAS Semiconductor Tracker*. Nucl. Instrum. Meth. A568 (2006), 642.
- [7] ATLAS Collaboration, *ATLAS Inner Detector Technical Design Report*, Volume 2, ATLAS TDR 5, CERN/LHCC/97-17, ISBN 92-9083-103-0.
- [8] P.Vankov, *ATLAS Upgrade for the HL-LHC: meeting the challenges of five-fold increase in collision rate*, arXiv:1201.5469v1 (2012).
- [9] D.Malon, E.May, A.Vaniachine, S.Resconi, J.Shank, S.Youssef, *Grid-enabled data access in the ATLAS Athena framework*.
- [10] A.Abdesselam *ATLAS Inner Deterctor Upgrade Simulation*.
- [11] G.Duckeck et. al.*ATLAS computing: Technical Design Report*, CERN public note.
- [12] Luehring, *Athena Pile-up Requirements*